ISBN: 978-3-95450-202-8 doi:10.18429/JACoW-HB2018-TUP2WA02

MOMENTUM SLIP-STACKING SIMULATIONS FOR CERN SPS ION BEAMS WITH COLLECTIVE EFFECTS

D. Quartullo*, T. Argyropoulos, A. Lasheen, CERN, Geneva, Switzerland

Abstract

The LHC Injectors Upgrade (LIU) Project at CERN aims at doubling the total intensity of the Pb-ion beam for the High-Luminosity LHC (HL-LHC) Project. This goal can be achieved by using momentum slip-stacking (MSS) in the SPS, the LHC injector. This RF gymnastics, originally proposed to increase bunch intensity, will be used on the intermediate energy plateau to interleave two batches, reducing the bunch spacing from 100 ns to 50 ns. The MSS feasibility can be tested only in 2021, after the beam controls upgrade of the SPS 200 MHz RF system, so beam dynamics simulations are used to design this complicated beam manipulation. Simulations of the MSS were performed using the CERN BLonD code with a full SPS impedance model. Attention has been paid to the choice of the RF and machine parameters (beam energy, time duration, RF frequency and voltage programs) to reduce losses and the final bunch length which is crucial for the injection into the LHC 400 MHz buckets. The initial beam parameters used in simulations were obtained from beam measurements in the first part of the SPS cycle taking into account bunch-by-bunch losses on flat bottom and development of bunch instabilities.

INTRODUCTION

The HL-LHC Project at CERN aims at doubling the peak luminosity of the Pb-ion beam after upgrade (2019-2021) [1]. To fulfil this requirement, the baseline of the LIU Project includes the decrease of the bunch spacing in SPS from 100 ns to 50 ns through momentum slip-stacking (MSS) [1]. This technique, already used in operation in Fermilab [2], allows two batches with slightly different momenta to slip relative to each other before being stacked one on top of the other. An RF voltage high enough to recapture the stacked bunches allows to double the bunch intensity at the end of the process. A variant of MSS is considered in the SPS: the two batches are not stacked on top of each other, but interleaved (see Fig.1). This provides the desired bunch spacing reduction while the bunch intensity remains unchanged.

MSS in SPS is potentially feasible thanks to the large bandwidth of the 200 MHz travelling-wave cavities (TWC) [3]. These will be divided into two groups and the RF frequency of each group will be tuned to one batch. Since independent LLRF controls for the two groups will be available only after upgrade, macro-particle simulations in the longitudinal plane are the only means to verify the MSS feasibility (alternative scenarios are being also considered [4]).

Preliminary simulations performed in 2014 showed promising results [5], however collective effects were not included and beam parameter variations along the batches were not taken into account. In the present work a more elaborated study is presented. Beam measurements provided realistic beam parameters which were used as initial conditions in simulations. Collective effects were included, using an accurate longitudinal impedance model. Machine and RF programs were designed to be used during and after MSS. Effort was spent to develop algorithms able to speed up the settings of the large number of parameters involved during MSS optimisation. The CERN BLonD macro-particle simulation code [6] has been used for the studies.

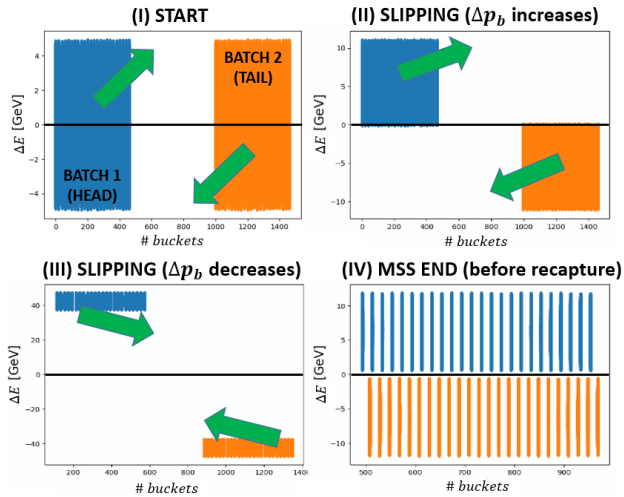

Figure 1: Example of planned MSS procedure in SPS. The two batches, starting from Phase I, move in longitudinal phase space relative to each other. The black line marks $\Delta E = E - E_0 = 0$, where E_0 is the design energy. In Phase II the distance in momentum Δp_b between the batches increases, while the opposite happens in Phase III. Recapture is done in Phase IV.

SLIP-STACKING PRINCIPLE

MSS is usually performed at constant magnetic field B_0. The design momentum p_0 is then defined by [7]

$$B_0 R_0 = p_0/q, \tag{1}$$

where q is the particle charge and the bending radius ρ of the dipole magnets has been approximated with the average machine radius R_0. Keeping the magnetic field constant and in linear approximation, the following relations hold [7]

$$\frac{\Delta\omega_{rf}}{\omega_{rf,0}} = -\eta_0 \frac{\Delta p}{p_0} = -\eta_0 \gamma_{tr}^2 \frac{\Delta R}{R_0}, \tag{2}$$

where $\omega_{rf} = 2\pi f_{rf}$ is the angular RF frequency, γ_{tr} is the relativistic gamma at transition energy and $\eta_0 = \gamma_{tr}^{-2} - \gamma_0^{-2}$ is the slippage factor. The design $\omega_{rf,0} = h\omega_0$ (with h the

* danilo.quartullo@cern.ch

Content from this work may be used under the terms of the CC BY 3.0 licence (© 2018). Any distribution of this work must maintain attribution to the author(s), title of the work, publisher, and DOI.

ISBN: 978-3-95450-202-8 doi:10.18429/JACoW-HB2018-TUP2WA02

harmonic number) can be derived from p_0, as well as the design γ_0. All the variables in Eq. (2) represent changes with respect to the corresponding design quantities. In a reference frame synchronised with the design revolution period T_0 (see Fig. 1), a variation $\Delta\omega_{rf}$ implies a change in the RF phase according to

$$\Delta\phi_{rf} = \frac{2\pi h \Delta\omega_{rf}}{\omega_{rf,0}}. \quad (3)$$

Taking as an example the case in Fig. 1 ($\eta_0 > 0$), the head batch will gain momentum when the RF frequency of the corresponding RF system is decreased. According to Eqs. (2) and (3) the batch will be displaced radially outwards while slipping to the right in phase. An analogous but opposite reasoning applies to the second batch.

The group of RF cavities not synchronized with the batch perturbs its motion. The severity of the perturbation is linked to the distance between batches in phase and momentum. The latter is described by the slip-stacking parameter [8]:

$$\alpha \doteq \frac{\Delta f_{rf,b}}{f_{s0}} = 2\frac{\Delta E_b}{H_b}, \quad (4)$$

where $\Delta f_{rf,b}$ and ΔE_b are the differences in RF frequency and total energy between the two batches, f_{s0} is the zero amplitude synchrotron frequency of the unperturbed bucket and H_b is half of the bucket height. When $\alpha = 4$, the separatrices of the two batches are tangent to each other. This value has been proven to be a lower limit for dynamic stability [8]. If $\alpha \gg 4$, the perturbation averages within a synchrotron period and its effect is less damaging. However a large α implies a higher RF voltage needed for recapture which leads to a larger emittance blow-up after filamentation. Phase IV in Fig. 1 shows a beam configuration where $\alpha = 4$.

MOMENTUM SLIP-STACKING IN SPS

LHC Pb-ion beam in SPS is currently accelerated from 17 GeV/qc ($\gamma = 7$) to 450 GeV/qc ($\gamma = 191$), where $q = 82$ is the number of protons per ion. Three different optics, called Q20, Q22 and Q26, are available in the SPS, depending on the working point adopted. In all cases, the beam energy crosses the transition energy during the first part of the ramp ($\gamma_{tr}^{Q20} = 18$, $\gamma_{tr}^{Q22} = 20$, $\gamma_{tr}^{Q26} = 23$). The Q20 optics is currently used in operation. The accelerating RF system is the 200 MHz TWC ($h = 4620$). For proton beams, a forth harmonic RF system (800 MHz) is used in addition to the main one to enhance Landau damping. However, this system is not used presently in operation with ion beams.

MSS Energy and SPS Momentum Program

The first choice to be made is the energy at which slip-stacking should be performed. At injection energy, the presence of relatively strong space charge, intra-beam scattering (IBS) and RF noise prevent us from applying MSS there. On the other hand at flat top all particles lost during the RF manipulations would be transferred to the LHC. For these reasons an intermediate energy plateau has been chosen (300 GeV/qc) which is quite far from the transition energy with a higher stability threshold compared to the top energy. Since only integer multiples of the CERN PSB cycle (1.2 s) can be added to the currently used SPS momentum program, the length of the plateau was chosen to be 1.2 s. Figure 2 shows the momentum program used in simulations. Out of 1.2 s, 0.8 s were used for MSS, while 0.4 s were utilized to let the bunches filament after recapture.

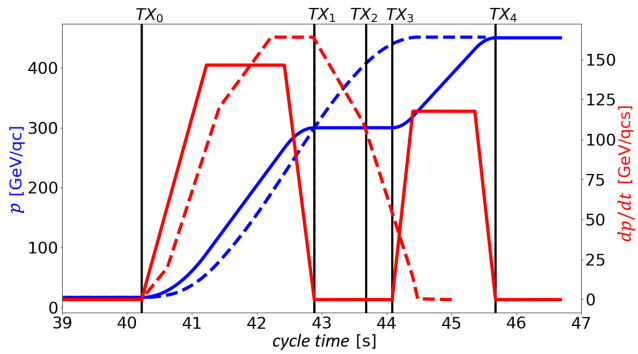

Figure 2: Operational (dashed) and used in simulations (continuous) momentum programs (blue) and their derivatives (red). The label TX_0 marks the ramp start, TX_1 the start of MSS, TX_2 the end of MSS, TX_3 and TX_4 the start and the end of the second ramp.

RF Perturbation and Initial Conditions

Every batch will contain 24 bunches spaced by 100 ns (assuming a 100 ns spacing between the mini-batches coming from the CERN PS). To limit the perturbation of the second RF system on each batch, the two independent 200 MHz groups are switched on only when the corresponding batch passes by. Figure 3 shows cavity voltage measurements for the currently available TWC [9]. The rising and decaying times are similar and ranging from 1 µs to 1.2 µs, depending on the cavity length. We expect that this time T_b^{th}, which currently relates to the 4 and 5-section cavities, will be lower during MSS, since the relatively low required voltage for this manipulation can be provided only by the new 3-section cavities. In simulations $T_b^{th} = 1$ µs was assumed.

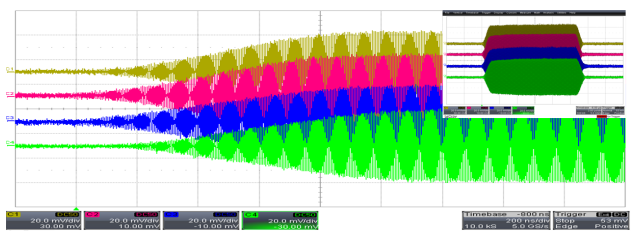

Figure 3: Measurements of cavity voltages for the currently used two 4-section (top) and two 5-section (bottom) TWC (the time division length is 2 µs) [9]. The top right image shows the RF voltage rise and decay during batch passage.

It is essential that $\alpha \gg 4$ when the distance between the batches T_b is equal to T_b^{th} (to minimize the perturbation effects). We assumed a relatively large $T_b = 2.7$ µs at TX_1,

Content from this work may be used under the terms of the CC BY 3.0 licence (© 2018). Any distribution of this work must maintain attribution to the author(s), title of the work, publisher, and DOI.

ISBN: 978-3-95450-202-8 doi:10.18429/JACoW-HB2018-TUP2WA02

Content from this work may be used under the terms of the CC BY 3.0 licence (© 2018). Any distribution of this work must maintain attribution to the author(s), title of the work, publisher, and DOI.

giving priority to the adiabaticity of the MSS manipulation. Figure 4 shows an example of α evolution during MSS.

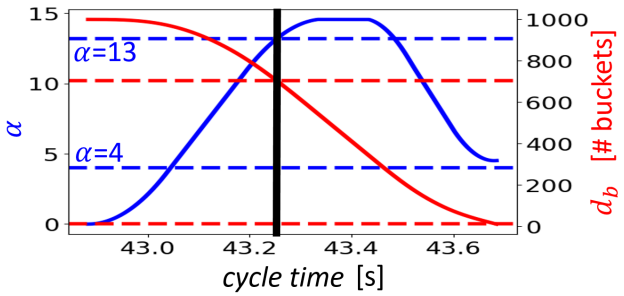

Figure 4: Example of α evolution during MSS ($\alpha_{TX_2} = 4.5$). The black line marks the time when $T_b = T_b^{th}$. The quantity d_b refers to the head-head distance between the batches. At TX_1 d_b = 1000 buckets (or T_b = 2.7 µs), while at TX_2 d_b = 10 buckets (bunch spacing at the end of MSS).

Beam measurements of the operational SPS ion cycle [10] were used to set the initial bunch distributions in simulations. Figure 5 shows that the emittance increases by a factor of 2 along 24 bunches in the SPS, whereas the intensity grows by a factor of 1.5 (this variability is due to continuous losses at flat bottom). An extrapolation was done to obtain the beam parameters for the 48 bunches needed for MSS. The emittance ϵ_l was calculated using the full-width-half-maximum bunch length rescaled to $4\sigma_{rms}$ of a Gaussian profile (convention used in SPS). However, as we will see, the bunch profiles obtained after MSS are not Gaussian but they have two peaks. For this reason the bunch length and emittance in the present paper will be determined by the portion of the line density containing 95% of the particles. The fact that in measurements losses happen gradually along the flat bottom indicates that there are strong tails in the bunches. For that reason a binomial distribution with μ=5 was used in the studies.

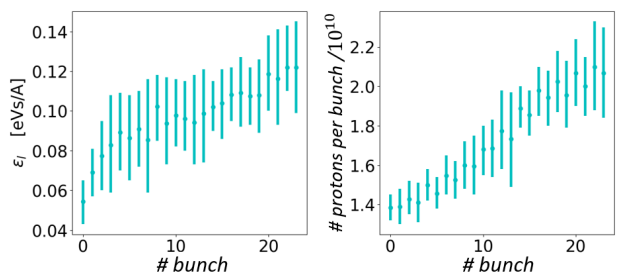

Figure 5: Measured longitudinal emittances and intensities along 24 bunches at 300 GeV/qc.

RF Programs During MSS

During MSS, we suppose that the RF frequency programs of the two 200 MHz RF subsystems are opposite relative to $\omega_{rf,0}$ ($\omega_{rf}^{(1)} + \omega_{rf}^{(2)} = 2\omega_{rf,0}$) and that the two RF voltage programs are equal ($V_{rf}^{(1)} = V_{rf}^{(2)}$). At recapture time TX_2 we have $\omega_{rf}^{(1)} = \omega_{rf}^{(2)} = \omega_{rf,0}$ and a common recapture voltage V_{rf}^{rc} is used. According to Eq. (2) the RF frequency programs determine the momentum programs applied to the two batches. The voltage program during MSS is computed for constant filling factor of bucket in energy q_e^{MSS} relative to the highest emittance bunch (see Fig. 6).

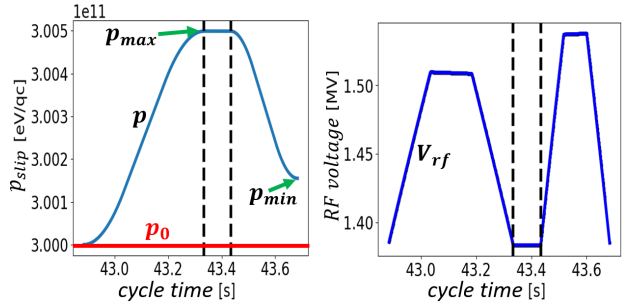

Figure 6: Example of momentum and RF programs for one batch during MSS (same case as in Fig. 4).

The calculation of the momentum program during MSS can be tedious when parameter scans have to be performed for optimization (see next Section) and accurate calibration has to be done case by case to avoid misalignments between the two batches before recapture. Automatic tuning to obtain alignment with arbitrary precision is necessary. Iterative algorithms have been conceived for this purpose, assuming constant emittance and filling factor during MSS.

RF Programs After MSS

The recapture voltage V_{rf}^{rc} is used during the filamentation process in $[TX_2, TX_3]$. Then, the filling factor in energy relative to the highest emittance bunch is computed in TX_3. The RF voltage program for the second ramp is calculated assuming this filling factor constant. At flat top, with a duration of 1 s, two options for beam transfer to LHC were examined (assuming a maximum available voltage of 15 MV [11]). Bunch compression, where the RF voltage in TX_4 is increased linearly and adiabatically for 0.5 s (or about 180 synchrotron periods) up to 15 MV and then is kept constant until extraction. Bunch rotation, where the RF voltage in TX_4 is used for 0.8 s, then it is increased non-adiabatically (few turns) to 15 MV and after a quarter of synchrotron period the beam is extracted.

ANALYSIS OF SIMULATION RESULTS

In this section, unless otherwise specified, simulation results with the currently used Q20 optics are presented. Given the considerable number of parameters in play and knowing the required constraints at LHC injection, parameter scans were made to find the best combinations. The following fundamental quantities were considered: filling factor q_e^{MSS} (from 0.45 to 0.9, step 0.05), α_{TX_2} (from 3.5 to 8, step 0.5), V_{rf}^{rc} (from 1 MV to 9 MV, step 0.5) and the type of RF manipulation at flat top (compression or rotation).

Two constraints were considered. The first refers to the maximum bunch length at the SPS extraction. This number τ_{max} has to be less than 1.65 ns, since larger bunch lengths

ISBN: 978-3-95450-202-8 doi:10.18429/JACoW-HB2018-TUP2WA02

lead to considerable losses when injected to the 400 MHz LHC RF buckets. The second constraint results from the total losses due to the MSS process. This value as defined by the LIU project should be less than 5% [4]. In the following simulations the total losses L_{tot} are defined by the sum of the particles lost in the SPS hitting the beam pipe (L_{SPS}) and the satellite particles which are formed in SPS during MSS and will be transferred to the LHC (S_{LHC}).

Bunch Compression

A combination A is optimal if there exists no other combination B for which $L^A_{tot} > L^B_{tot}$ and $\tau^A_{max} > \tau^B_{max}$. The simulation results with collective effects are shown in Fig. 7 for bunch compression, together with the optimal solutions. Essentially no combination is acceptable, so bunch compression at flat top cannot be adopted. The maximum emittance ϵ_{max} after filamentation should be lower than 0.32 eVs/A to have $\tau_{max} < 1.65$ ns. From Fig. 7 one can see that the real limitation is on τ_{max} (or ϵ_{max}) rather than on L_{tot}. In other words the losses can be almost arbitrarily reduced increasing for example α_{TX_2} and V^{rc}_{rf} while decreasing q^{MSS}_e (and on average we would obtain $\tau_{max} \approx 2$ ns). On the other hand, mostly because of the lower stability limit for α_{TX_2}, it is difficult to have arbitrarily low emittances after filamentation, unless considerable losses are allowed.

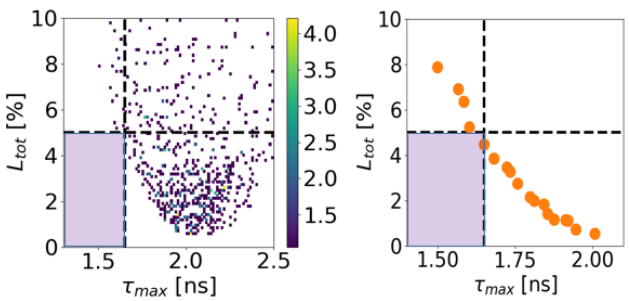

Figure 7: Simulation results (bunch compression) in the L_{tot}-τ_{max} plane (left). The optimal solutions are on the right. The purple area indicates where the constraints are satisfied.

Bunch Rotation

Results for the bunch rotation case are shown in Fig. 8. The average τ_{max} shifts from 2 ns to 1.6 ns, allowing numerous combinations to satisfy the constraints. Considering the optimal solutions and giving priority to losses reduction while keeping some safety margin for τ_{max}, the green dot marks the proposed solution, with $\alpha_{TX_2} = 4.5$, $q^{MSS}_e = 0.65$ and $V^{rc}_{rf} = 8$ MV. The relatively low q^{MSS}_e and α_{TX_2} slightly higher than 4 allow to have low $L_{tot} = 0.43\%$, $S_{LHC} = 0.13\%$ and $L_{SPS} = 0.30\%$.

The feasibility of this solution was verified. The maximum radial displacement for one batch during MSS was 5.67 mm and 7.8 mm if the spread in energy is included (the current one-sided aperture limitation is around 20 mm). The maximum RF frequency spread during MSS was 1 kHz, three orders of magnitude lower than the RF cavity bandwidth. As for the peak RF voltage, the maximum value during MSS was only 1.54 MV (for one subsystem) and during acceleration to flat top it reached 14.6 MV, still inside the limitations (see also Figs. 4 and 6 which refer to this optimal solution).

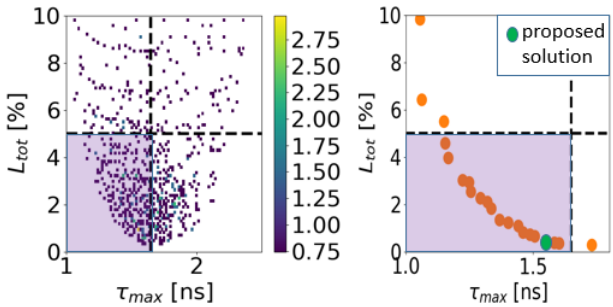

Figure 8: Simulation results (bunch rotation) in the L_{tot}-τ_{max} plane (left). The optimal solutions are on the right. The purple area indicates where the constraints are satisfied.

Figures 9 and 10 show all the significant parameters involved. The green lines mark the chosen combination. Qualitatively, as τ_{max} increases, we can see that L_{tot}, S_{LHC} and L_{SPS} decrease while ϵ_{max} increases. In addition, α_{TX_2} remains constant, q^{MSS}_e decreases and V^{rc}_{rf} increases.

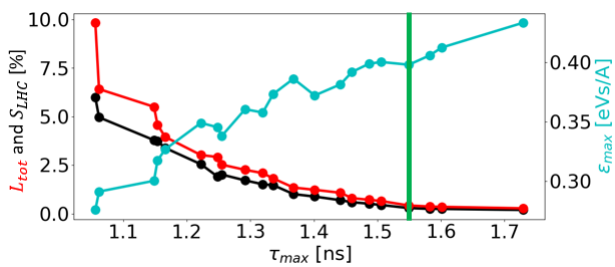

Figure 9: Total losses, satellites (L_{tot}, S_{LHC}) and emittance (ϵ_{max}) as a function of τ_{max} for the optimal solutions in Fig. 8. The green line marks the proposed combination.

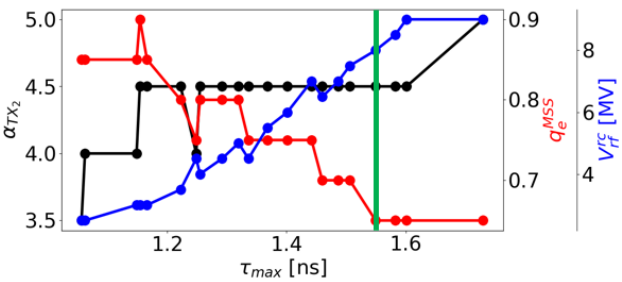

Figure 10: Parameters α_{TX_2}, q^{MSS}_e and V^{rc}_{rf} as a function of τ_{max} for the optimal combinations shown in Fig. 8. The green line marks the proposed combination.

It is expected that all the optimal solutions have $\alpha_{TX_2} \approx 4$, since 4 is the lower limit for stability and larger values would make the solutions not optimal. However $\alpha_{TX_2} \approx 4.5$ gives some safety margin to soften the impact of the chaotic motion

Content from this work may be used under the terms of the CC BY 3.0 licence (© 2018). Any distribution of this work must maintain attribution to the author(s), title of the work, publisher, and DOI.

ISBN: 978-3-95450-202-8 doi:10.18429/JACoW-HB2018-TUP2WA02

Content from this work may be used under the terms of the CC BY 3.0 licence (© 2018). Any distribution of this work must maintain attribution to the author(s), title of the work, publisher, and DOI.

close to $\Delta E = 0$ since the highest emittance bunches fill almost the full bucket even for low q_e^{MSS}.

Qualitatively, Figs. 9 and 10 are explained below. Going from an optimal combination A to another optimal combination B with $\tau_{max}^B < \tau_{max}^A$ ($\epsilon_{max}^B < \epsilon_{max}^A$) it follows that $V_{rf}^{rc,B} < V_{rf}^{rc,A}$, since the bucket area after recapture has to decrease. To avoid losses in SPS due to particles outside the separatrix of the recapture bucket, one needs $\Delta E_b^B < \Delta E_b^A$. Since α_{TX_2} is roughly constant, the RF voltage $V_{rf,u}$ of the unperturbed bucket of one of the two batches has to decrease ($H_b \propto V_{rf,u}^{1/2}$). The peak energy spread of the bunch inside the unperturbed RF bucket $\widehat{\Delta E}$ decreases as well ($\widehat{\Delta E} \propto V_{rf,u}^{1/4}$) and thus $q_e^{MSS,B} > q_e^{MSS,A}$. A higher q_e^{MSS} implies larger L_{SPS}. Since the bunch is now closer to the axis $\Delta E = 0$, where the chaotic motion is more significant, $S_{LHC}^B > S_{LHC}^A$. Finally $L_{tot}^B > L_{tot}^A$.

Figure 11 shows the optimal combinations neglecting intensity effects. No significant differences can be noticed, implying that intensity effects do not enhance instabilities which would increase the total losses or blow up the beam.

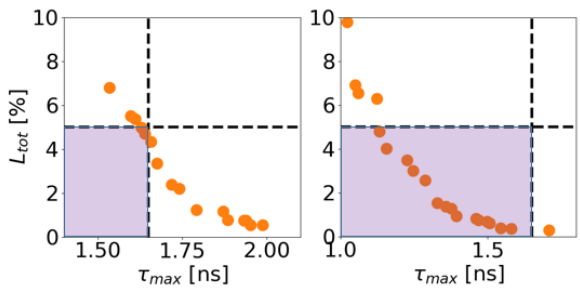

Figure 11: Optimal combinations for the bunch compression (left) and rotation (right) cases without intensity effects.

The two other optics, Q22 and Q26, were also analysed (Fig. 12). Because of the lower slip factor, a slightly higher p_{max} during MSS was needed (keeping constant the time duration). The radial displacement was still inside the aperture limitations and the process was adiabatic. Fixing all the other parameters, a lower slip factor implies a lower q_e^{MSS} which helps in reducing L_{SPS}. The bucket area after recapture decreases as well and this implies a lower τ_{max}. Bunch compression could be adopted if the Q22 (or even better the Q26) optics is chosen, however these optics are more sensitive to IBS and transverse space charge effects.

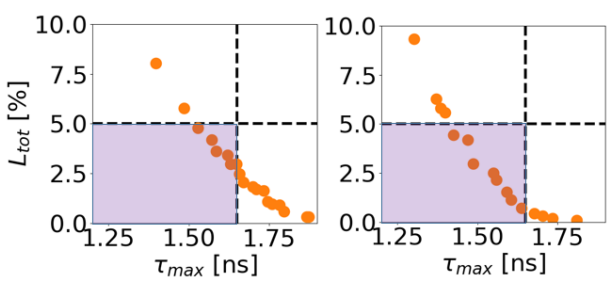

Figure 12: Optimal combinations (compression case) for the Q22 (left) and Q26 (right) optics with intensity effects.

Loss of Landau Damping During MSS

Even if intensity effects do not influence the losses and bunch length, loss of Landau damping was observed: the dipole oscillations due to the RF perturbation during MSS remain up to flat top, being stronger for shorter bunches.

Taking as an example the proposed solution found previously, Fig. 13 shows that dipole oscillations at flat top are higher by two order of magnitudes with intensity effects. The hollow bunch which is formed after recapture filaments perfectly without intensity effects, while a very dense island appears with intensity effects. From Fig. 13 it can be seen that the shortest bunches are the most affected.

Rise of dipole oscillations could be damped by phase loop. In addition, the 800 MHz system could be used to increase the non-linearities of the bunch and make the island in phase space filament. However, simulations using the 800 MHz RF system did not show significant improvement. This can be attributed to the special hollow distribution of the bunches after MSS. Further studies are ongoing.

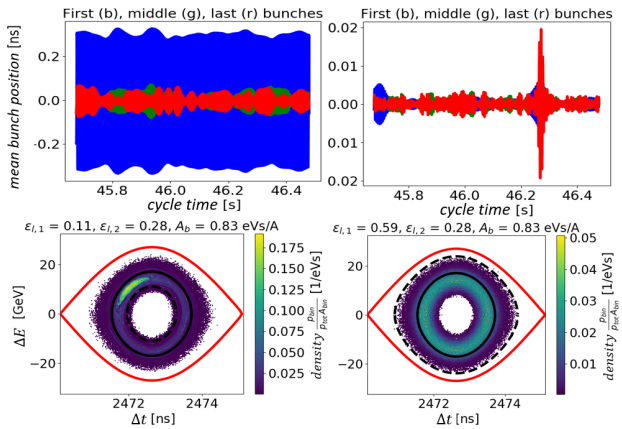

Figure 13: Beam quality with (left) and without (right) intensity effects. Top: bunch positions at flat top for the first (blue), middle (green) and last (red) bunches. Bottom: phase space of the first (smallest) bunch at beginning of flat top.

CONCLUSION

Momentum slip-stacking for LHC ion beams in SPS after LIU upgrades is fundamental to fulfil the requirements imposed by the High Luminosity LHC Project. In this paper the optimum parameters involved in this complicated beam manipulation were suggested. Simulations using the SPS impedance model showed that MSS can be applied under certain conditions, providing at extraction the beam parameters (τ_{max}, intensity) required by the LIU project. However, loss of Landau damping was observed and further studies are needed to find possible cures.

ACKNOWLEDGEMENTS

We would like to thank E. Shaposhnikova for her precious support. Important help was given by our colleagues H. Bartosik, P. Baudrenghien, T. Bohl, K. Iliakis, J. Repond and G. Rumolo.

ISBN: 978-3-95450-202-8 doi:10.18429/JACoW-HB2018-TUP2WA02

REFERENCES

[1] J. Coupard, H. Damerau, A. Funken, R. Garoby, S. Gilardoni, B. Goddard, K. Hanke, D. Manglunki, M. Meddahi, G. Rumolo, R. Scrivens, and E. Shaposhnikova, "LHC Injectors Upgrade, Technical Design Report, Vol. II: Ions," Tech. Rep. CERN-ACC-2016-0041, CERN, Geneva, Apr 2016.

[2] J. Eldred, "Slip-Stacking Dynamics for High-Power Proton Beams at Fermilab." PhD thesis, 2015.

[3] G. Dome, "The SPS Acceleration System Travelling Wave Drift-tube Structure for the CERN SPS," tech. rep., 1977. CERN-SPS-ARF-77-11.

[4] A. Saa Hernandez, "Results from ion studies in PS and SPS from 2016/2017 and planning for 2018." presentation at the CERN Injector MD day, 2018.

[5] T. Argyropoulos, T. Bohl, and E. Shaposhnikova, "Slip stacking in the SPS." presentation at the CERN LIU day, 2014.

[6] "CERN BLonD code." http://blond.web.cern.ch.

[7] C. Bovet *et al.*, "A Selection of Formulae and Data Useful for the Design of A.G. Synchrotrons," CERN-MPS-SI-INT-DL-70–4, 1970.

[8] F. E. Mills, "Stability of Phase Oscillations Under Two Applied Frequencies," 1971.

[9] T. Bohl. CERN, personal communication, 2018.

[10] A. Lasheen, "Beam Measurements of the Longitudinal impedance of the CERN Super Proton Synchrotron." PhD thesis, 2017.

[11] E. Shaposhnikova *et al.*, "Upgrade of the 200 MHz RF System in the CERN SPS," in Proc. 2nd Int. Particle Accelerator Conf. (IPAC11), San Sebastian, Spain, Sep. 2011, paper MOPC058, pp. 214-216.

Content from this work may be used under the terms of the CC BY 3.0 licence (© 2018). Any distribution of this work must maintain attribution to the author(s), title of the work, publisher, and DOI.